Transient flow analysis inside a skirted Jack-up's foundation towards the outside seabed

Siamak Feizi* and Knut Arnesen
Foundations group, DNV GL, Norway

Ovar Aarsland
Statoil ASA, Norway

* *corresponding author siamak.feizi@dnvgl.com*

ABSTRACT
In the soil-structure interaction analyses the moment restraint is usually calculated as if the spudcan foundation has an ideal contact with the soil. However, full contact might not be achieved. Water-filled pockets may be present between the foundation base and the seabed. If the soil behaves undrained for the transient wave loading, loads will be transferred directly as increased pressure in the water pockets and further as pore pressures in the soil underneath. To investigate the possibility of initiating piping in the soil outside one of the spudcan foundations during storm loading, a series of FEM analysis were performed for a Jack-up with skirted foundation. When the foundation is loaded in compression, suction is generated in the closest vicinity outside of the foundation in the pore water. This suction prohibits piping initiating around the skirts. Further away from the foundation, high hydraulic gradients occur toward the seabed and the soil may become liquefied, but for a very short time, thus, it is not foreseen that any soil will be eroded. A basic assumption for the analyses is that there is no initial piping as a result of installation.

KEY WORDS: Transient flow, Jack-up foundation, piping

INTRODUCTION
Mobile jack-up rigs with the skirted spudcan foundation are widely used in offshore oil and gas exploration and a steadily increasing trend for their use in deeper and harsher conditions is expected [1] and [2]. A jack-up rig is typically supported by three or occasionally four legs.
The foundation penetration, punch-through phenomenon, footprint effects and spudcan fixity are the most interesting topics for researches in this field. In most cases, the moment restraint is calculated as if the foundation has an ideal contact with the soil. Thus, full penetration has been assumed in those stiffness analyses. However, full contact might not be achieved because of a combination of possible incomplete penetration of skirts, uneven and/or sloping seabed and uneven foundation base, as well as limited ability to fill all voids by local squeezing of soil during preloading. Thus, water-filled pockets will normally be present between the foundation base and the seabed. In a storm situation, the vertical reaction due to a combination of vertical force and moment will be significantly higher than during preloading. If the soil underneath the foundation behaved drained for the short term loading, in addition to the flexibility due to the global drained response of a foundation in ideal contact with the soil, additional flexibility would result from local squeezing of soil to fill voids. If the soil behaves undrained short term loading will be transferred directly as increased pressure in the water pockets and further as pore pressures in the soil underneath. This will cause a transient pore water flow out of the foundation towards the seabed. If critical gradients occur near the seabed, this might lead to piping in the soil. Piping would then allow water to flow back and forth from the water-pockets with resulting increased rotation and correspondingly reduced moment restraints. Great efforts have been made to identify the pore pressure response during spudcan penetration by Dean [3] and Zhou [4]. However, the spudcan footing is assumed to be wished-in-place at prescribed depth, which turns out to be small strain problem and cannot model the real large soil deformation by continuous spudcan penetration [9]. A few other studies in this field can be found in [5] to [9] as examples. It is tried in this paper to highlight the possibility of initiating piping in the soil outside of the spudcan foundations during storm loading. The Mariner jack-up (Statoil) and one of its spudcan foundations are selected in our study. A series of Finite Element (FE) analysis by means of PLAXIS 2D [7] are performed to investigate this phenomenon.

METHODOLOGY AND ANALYSES DETAILS

Rather than analyzing the complex 3D situation of moment loading on a foundation with irregularly distributed water pockets, the problem was simplified to an axisymmetric situation with vertical loading on a skirted foundation with a continuous thin water pocket underneath the foundation. Since a trapped water pocket cannot be modelled directly in PLAXIS, this is simulated as a thin soil layer with high permeability. Furthermore, since the peak load from the wave loading lasts only a fraction of the wave period (T), conservatively assumed to be around T/3 to T/4, only the results of the first 6 seconds are presented.

Foundation geometry

A Schematic model of the Mariner Jack-up and Leg chord and leg side name convention are shown in Figure 1. A cross section of the skirted spud-can foundation is shown in Figure 2. The foundation structure has a hexagonal footprint, which is simulated by a circular area with diameter 21.6 m. The foundation structure is equipped with circumferential skirts to a level of 2 m below the lowest points of the base structure and 6 radial skirts to a level of 1 m below the lowest points of the base structure. Skirts are used in order to increase the foundation capacity in general.

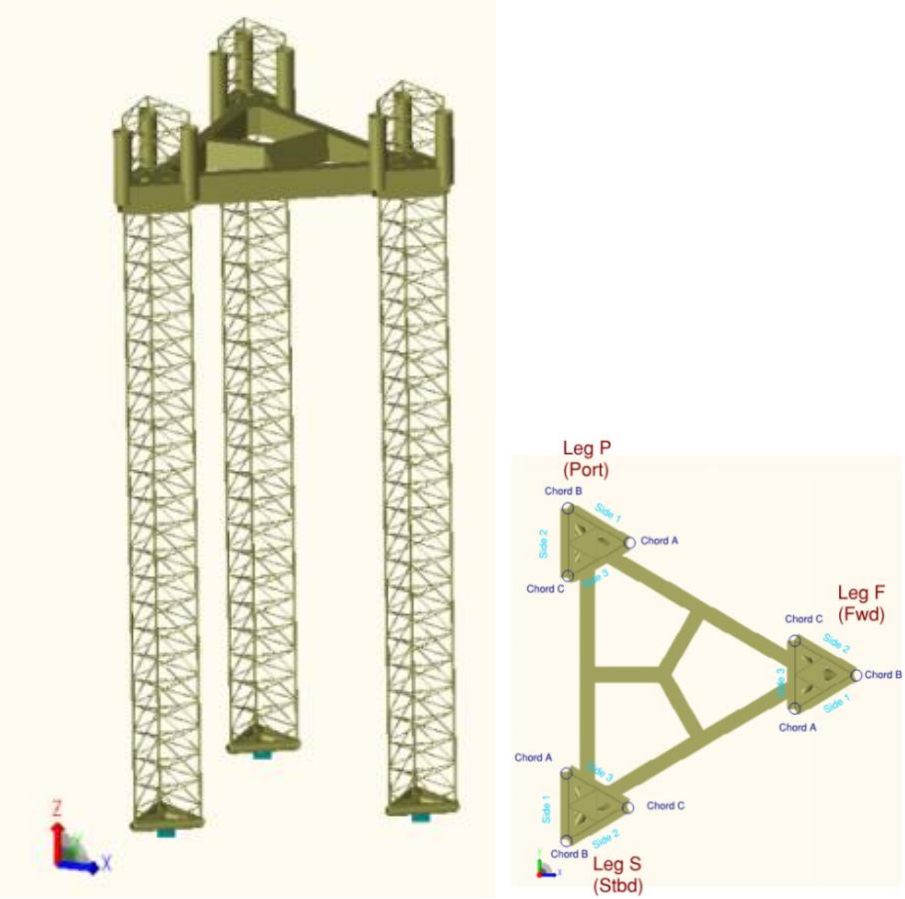

Figure 1 Structural Model CJ70-X150-ST and leg chord and leg side name convention at Mariner

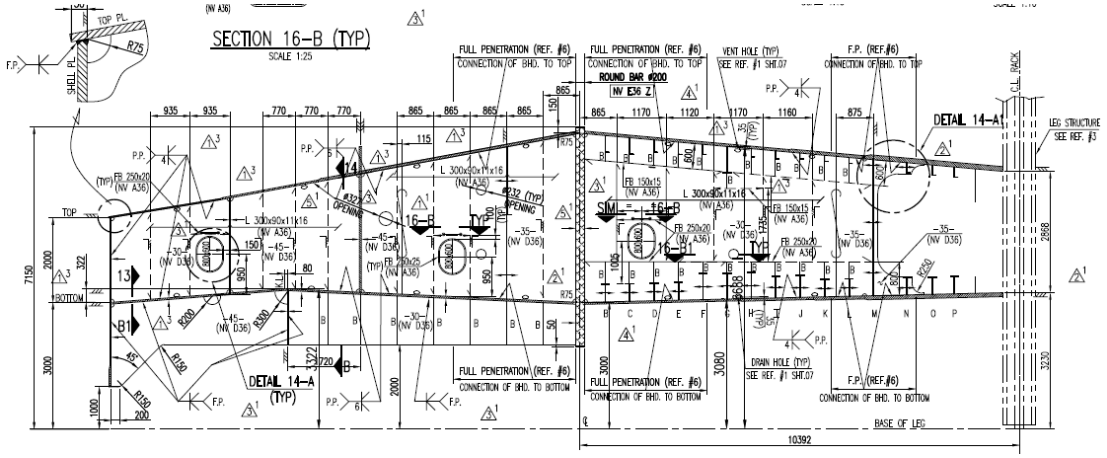

Figure 2 Skirted spud-can foundation

Loads

The initial stress conditions are established by use of the K_0'-procedure in the PLAXIS model [7]. The installation of the Spudcan with its self-weight, corresponding to a distributed load of 315 kPa, is assumed to cause drained soil behavior. An operational distributed load of 250 kPa is applied on the spudcan foundation in the PLAXIS analyses to simulate the vertical stress close to the periphery corresponding to moment and additional vertical load from the storm loading as shown below:

Soil conditions

From seabed and downwards, the soil consists of 8 m sand overlying 17 m clay down to bedrock at 25 m depth. The sand consists of three layers and the clay consists of two layers shown in Figure 3. In PLAXIS, the three sand layers are represented by one equivalent sand layer as seen from the geometry model in Figure 4. In PLAXIS, it is not possible to model a trapped water pocket below the spudcan foundation, in which excess pore pressure is generated during undrained loading, without applying a soil cluster. Thus, a dummy sand layer was introduced in PLAXIS to model such a trapped water pocket. The effect of the soil skeleton was reduced as much as possible by applying a small bulk modulus (oedometer modulus) of the soil skeleton and a large coefficient of permeability. Thus, the compressibility is governed by the high bulk modulus of the pore water during undrained loading and the hydraulic potential will be close to constant through this layer during consolidation.

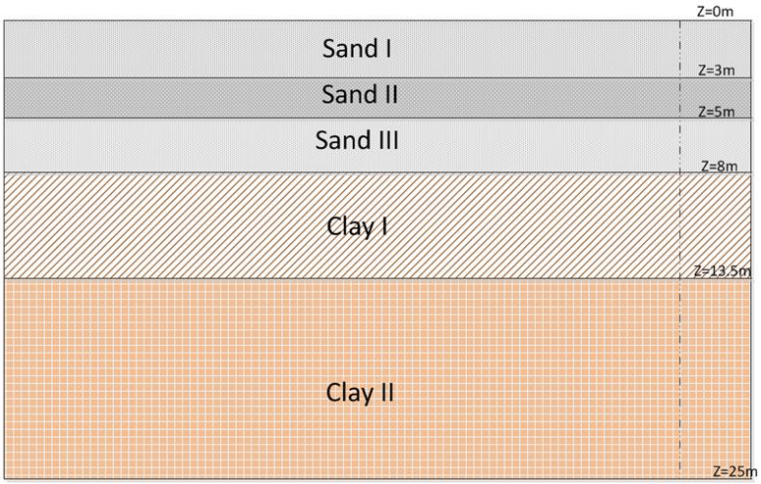

Figure 3 Soil layers

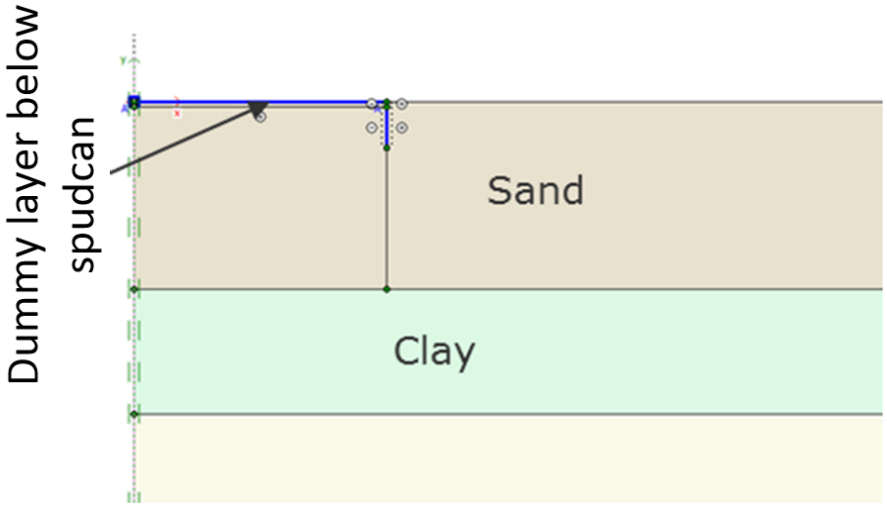

Figure 4 A part of the axial-symmetric geometry model in PLAXIS

In this study, soil deformations and global bearing capacity of the spudcan are not considered. Therefore, the hydraulic properties of the soil have been the main focus, while the stiffness and strength parameters are less emphasized. The transient pore water flow is likely to occur in the sand, since it is much more permeable than the underlying clay. Thus, the modelling of the sand layer is emphasized and the parameter study is limited to a variation of the parameters and modelling of this layer.
The sand is modelled by use of the elasto – plastic Hardening Soil Model (HSM), while the two clay layers are modelled by use of the linear elastic perfectly-plastic Mohr-Coulomb Model (MCM). These soil models, input parameters and features are presented in Table 1. The sand is assumed to have a positive dilatancy angle, ψ = 8°. The Mohr Coulomb Model has been used for the clay layers. The soil parameters are specified in Table 1.

Table 1 Sand parameters for the Hardening Soil Model

Material	Drainage Type	c (kPa)	ϕ (°)	ψ (°)	E_{oed}^{ref} (MPa)	Permeability k (m/s)
Dummy layer	Drained	4	38	0	1	10
Dummy layer	Undrained (A)	4	38	0	1	10
Sand	Drained	4	38	8	35	0.1E-3
Sand	Undrained (A)	4	38	8	35	0.1E-3

Clay parameters for the Mohr Coulomb Model

Material	Drainage Type	c (s_u) (kPa)	ϕ (°)	ψ (°)	E_{oed} (MPa)	Permeability k (m/s)
Clay I	Undrained (B)	140	0	0	50	0.05E-9
Clay II	Undrained (B)	540	0	0	200	0.05E-9

In the coupled consolidation analyses, the time dependent behaviour and potential fall through the soil are mainly governed by the coefficient of consolidation, $C_v = E_{oed} \cdot k/\gamma_w$. The time needed to end the process of primary consolidation can be estimated as $t_p = H^2/C_v$, where H is the length of the drainage path. In the PLAXIS analyses, we have specified a constant coefficient of permeability, while the oedometric modulus E_{oed} of the sand varies with the effective stress level. Thus, E_{oed} varies both within the model and with the time of consolidation, and so does the C_v of the sand. E_{oed} and C_v are larger below the foundation than outside the skirt, since the effective stresses are higher. The trapped water in the pockets inside the spudcan is supposed to have a constant excess pore pressure. The coefficient of consolidation for this dummy layer is much higher than for the sand due to the much higher permeability modelled for the dummy layer. A C_v of 1000m^2/s results, compared to a C_v of 0.35m^2/s at a reference effective stress level of 100kPa for the sand.

Details of FEM model

The Spudcan and skirts are modelled by use of elastic plate elements with infinitely high stiffness, while the soil is modelled by use of 15 noded, triangular elements in PLAXIS 2D axisymmetric. The interface between the spudcan foundation and soil is modelled by use of interface elements. The boundaries are located far enough from the Spudcan not to interfere on the local Spudcan behaviour.

The initial stress conditions before installation of the Jack-up are established by use of the K_0-procedure in PLAXIS. After that, the following calculation phases are performed :

1. The spudcan foundation is installed by activating an equivalent skirted foundation that is very stiff and weightless.
2. The spudcan foundation is loaded corresponding to still water conditions, σ_{p0}, in drained soil conditions
3. The spudcan foundation is loaded with additional loads in undrained conditions from waves during storm loading, $\Delta\sigma_p$. The undrained behaviour of the sand is modelled by use of an undrained effective stress analysis with Drainage type = Undrained (A), while the undrained behaviour of the clay is modelled by use of an undrained effective stress analysis with Drainage type = Undrained (B). Excess pore pressures, Δu are generated. Conservatively the full load simulating the maximum pressure due to wave loading is applied in one step at t=0, thus not accounting for the time required to reach the maximum load.
4. After the undrained loading, a coupled consolidation analysis is performed in PLAXIS to model the transient flow caused by the storm induced excess pore pressures underneath the base of the spud-can foundation. Since the sand is much more permeable than the clay, the transient flow mainly takes place in the sand. Thus, focus has mainly been on the sand.

Since the sand layer has the main role in the current analysis, the modelling of the sand layer is emphasized and the parameter study is limited to a variation of the parameters and modelling of this layer. The parametric study performed in PLAXIS is summed up in Table 2.

Table 2 Parametric study cases

Analysis number	**Comment**
Analysis # 1	A model with soil parameters as presented in Table 1. The tension cut-off value is set to 0. The cavitation cut-off is not activated.
Analysis # 2	Same as analysis # 1, but the allowable tensile effective stress (tension cut-off) is increased to 5 kPa.
Analysis # 3 (Reference analysis)	Same as analysis # 2, but with cavitation cut-off at 1100 kPa. (The hydrostatic pressure at seabed was 1000kPa)
Analysis # 3.1	Same as analysis # 3, but with ten times higher coefficient of permeability for the sand, $k_{3.1}=10k_3$.
Analysis # 3.2	Same as analysis # 3, but with ten times lower coefficient of permeability for the sand, $k_{3.2}= k_3/10$.
Analysis # 4	Same as analysis # 3, but the total loading is reduced from 565 kPa to 400 kPa by reducing the undrained load from 250 to 85 kPa.

Analysis # 4.1	Same as analysis # 3, but the total loading is reduced from 565 kPa to 500 kPa by reducing the undrained load from 250 to 185 kPa.
Analysis # 4.2	Same as analysis # 3, but the total loading is increased from 565 kPa to 700 kPa by increasing the undrained load from 250 to 385 kPa.
Analysis # 5	Same as analysis # 3, but the drained loading is increased from 315 kPa to 450 kPa.

Analyses # 1, 2 and 3 are performed to look into the effect of tensile stresses in the sand in the PLAXIS analyses. The tension-cut off option in PLAXIS is used to limit tensile effective stresses and the cavitation cut-off option is used to limit pore water suction in the PLAXIS analyses. These features in PLAXIS are further explained in [7]. Analysis # 3 is considered to be the most realistic and relevant analysis. In this reference analysis, the effective tensile stresses in the sand are limited to the attraction value, $a=c/\tan\phi= 5$ kPa and the suction occurring in the sand is limited to the atmospheric pressure plus the water pressure at seabed, $\sigma_{atm}+H_w\gamma_w=100+100\cdot10=1100$kPa.

The allowable suction is corrected with $H_w\gamma_w$ since the water level for simplicity is lowered to seabed in the PLAXIS analyses. Analyses # 3.1 and 3.2 are performed to look into the effect of a variation of the coefficient of permeability of the sand, while analyses # 4, 4.1, 4.2 and 5 are performed to look into the effect of a variation of the drained and undrained loading of the spudcan.

ANALYSES RESULTS

Tensile stresses

Soil can sustain only small tensile effective stresses. This behaviour can be included in PLAXIS analyses by specifying a ‘’Tension cut-off’’ with an allowable tensile effective stress, σ_t. The value is by default taken equal to zero. This default value is used in analysis # 1. During drained loading in the PLAXIS analyses, the effective stresses change, but the tensile effective stresses are limited by the tension cut-off specified. Thus, large zones with tension cut-off points are observed as white spots near the seabed in the FEM model for analysis # 1 in Figure 5 (left). During additional undrained loading, most of the load is expected to be taken by increased pore pressure. However, effective stress changes are expected due to dilatancy during sharing as can be seen from Janbu’s pore pressure formula $\Delta u = \Delta\sigma_m - D\cdot\Delta\sigma_d$ or $\Delta\sigma_m' = D\cdot\Delta\sigma_d$, where the D-parameter represents dilatancy during sharing, and $\Delta\sigma_d$ and is the deviatoric stress. Since the dilatancy induced changes of the effective stresses are limited by the specified tension cut-off in the PLAXIS analysis, the zones with tension cut-off points are observed to spread out towards the spudcan and towards the right hand boundary as seen as white spots in the FEM model for analysis # 1 in Figure 5 (right). In the consolidation phase, the specified tension cut-off at zero effective tensile stress might influence the hydraulic gradients in the analysis. Since the calculated hydraulic gradient from analysis # 1 does not exceed 1.0 this could be an effect of tension cut-off at zero effective tensile stress, all other analyses were performed with an allowable effective tensile stress equal to the attraction $a=c/\tan\phi=5$ kPa of the sand.

The occurring suction in the model is limited by use of the ‘’Cavitation cut-off’’ option in PLAXIS in analyses # 3, 4 and 5. Normally, it is limited to the atmospheric pressure of 100 kPa. However, since the water level (H_w) is located at around 100m above seabed and for simplicity is lowered to seabed in the PLAXIS model, the cavitation cut-off is set equal to $H_w\gamma_w + \sigma_{atm} = 100*10+100= 1100$ kPa.

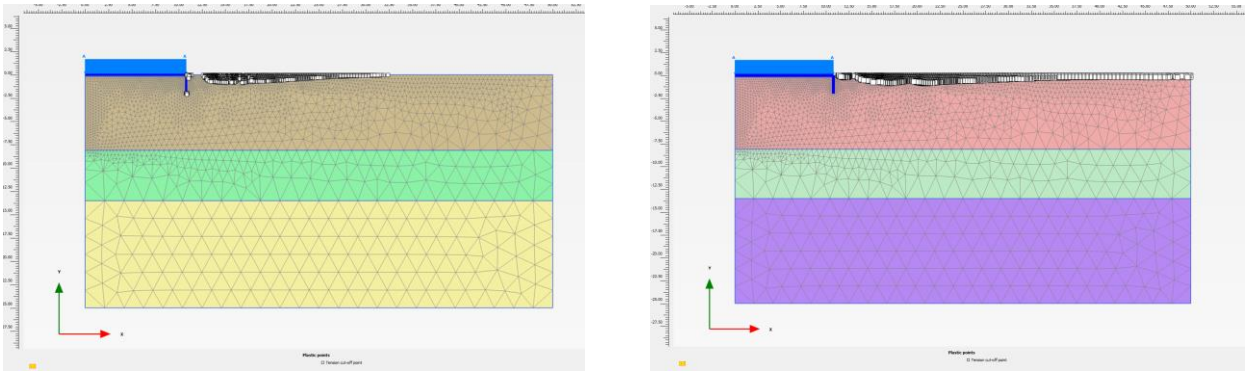

Figure 5 Tension cut-off points left) after drained loading, right) after undrained loading (analysis # 1)

Pore pressures

Excess pore pressures due to loading are presented for the reference analysis (analysis # 3). Since the maximum load is considered to last for approximately 1/3 to 1/4 of a wave period, which is around 10-15s, the main focus here is the time period between t=0 and t=4s. Figure 6 through Figure 8 show the excess pore pressure contours for the different calculation phases of the PLAXIS analysis. The pink coloured areas are those where the pore pressure falls outside the manually set limits of the scaling, here set to 0 and 50 kN/m^2.. The excess pore pressure contours from the analysis shows that excess suction (relative to hydrostatic) is created in a zone outside the skirt as a result of the downward motion of the foundation. This contributes to avoid critical gradients just outside the foundation.

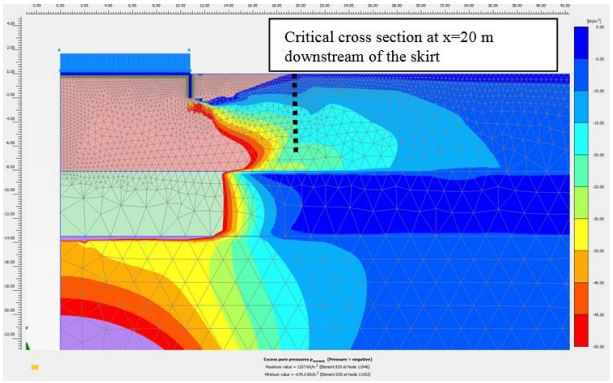

Figure 6 Undrained loading - t=0 (analysis # 3)

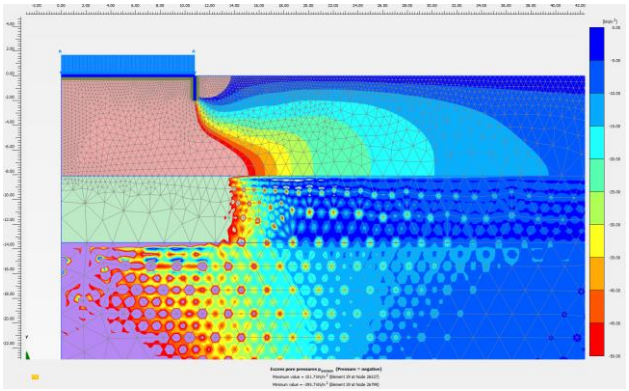

Figure 7 Consolidation phase - t=2s (analysis # 3)

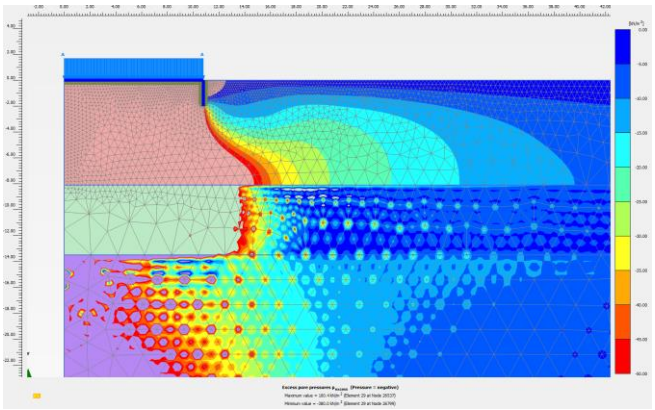

Figure 8 Consolidation phase - t=4s (analysis # 3)

Hydraulic gradients

For the reference analysis (analysis #3), the distribution of excess pore pressure shows that the hydraulic gradient towards the seabed is highest at a cross section at around x=20 m (approxinately 10 m from the spudcan edge). Therefore for evaluation of the risk of hydraulic fracturing, the value of the hydraulic gradient using the excess pore pressure values at x=20m is presented.

To calculate the hydraulic gradient (i), the following relation is used:

$$i = \frac{\Delta h}{l} = \frac{\Delta u / \gamma_w}{l} \tag{1}$$

where

Δh is the potential head, l is the distance measured along the flow line and Δu is the differential excess pore pressure.

In Figure 9, the depth distribution of the excess pore pressure down to a depth of 1 m below seabed is presented for the cross section at x=20 m for analysis #3.

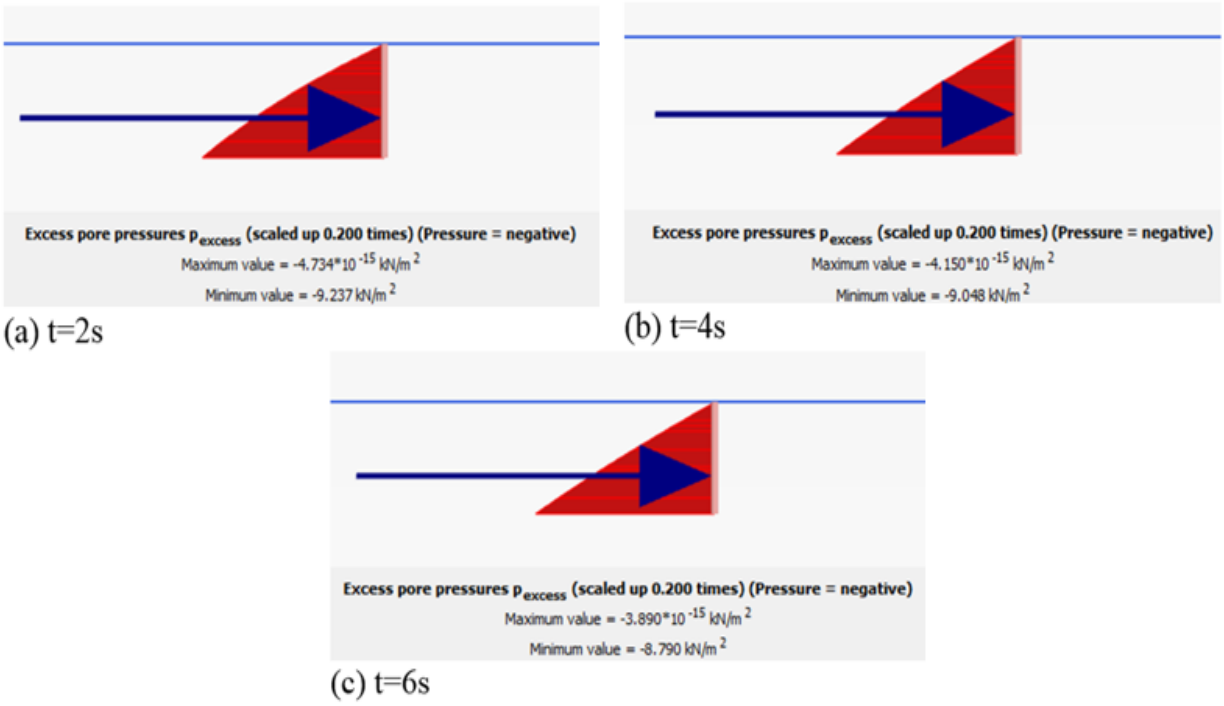

Figure 9 Depth distributions of excess pore pressure at x=20 m (analysis # 3)

A summary of the depth profiles of the hydraulic gradient at x=20 m for different times of consolidation is presented for the reference analysis in Figure 10. A critical hydraulic gradient of 1.0 is showed in the same figure. The depth profile at t=2s show a hydraulic gradient larger than 1.0 down to ca. 0.8m and the depth profile at t=4s show a gradient larger than 1.0 down to ca. 0.5m. After 6s of consolidation, the hydraulic gradient is below the critical value of 1.0 for all depths. This development over time is caused by dissipation of the excess pore pressure. The gradients presented for the undrained stage at t=0s are the start point of the transient flow that will take place in the next consolidation phases.

Figure 11 shows the hydraulic gradients from all the listed analyses in Table 2. The comparison is solely done for t=2s because Figure 10 showed that the highest hydraulic gradients are expected to be observed just after the initiation of the consolidation process in the analyses. It is found that in the consolidation phases of analysis # 1, the tension cut-off at zero effective tensile stress results in hydraulic gradient smaller than 1.0, apart from at t=0 in the upper 20-30cm. Also, the hydraulic gradients from analyses # 2 and # 3 are almost identical.

In analyses # 4, 4.1 and 4.2, the effects of a variation of the loads in undrained condition are investigated. As seen in Figure 11, analysis # 4.2 gives almost the same hydraulic gradient as analysis # 3, while analyses # 4 and # 4.1 show smaller hydraulic gradients than the reference analysis. Thus, the parametric study shows that a reduction of the undrained load, leads to a reduction of the hydraulic gradient in the analyses outside the foundation. The main reason might be that smaller excess pore pressure is generated underneath the spudcan due to smaller total load. However, after reaching a certain excess pores pressure underneath the spudcan with time of consolidation, a further increase of the undrained load would not increase the hydraulic gradient. A comparison of the results of analysis # 4.2 with the results of the reference analysis shows this.

Effects of varying the drained load are investigated in analysis # 5. Comparison of the results from this analysis with the results from analysis # 3 shows that such a variation of the drained load has limited impact on the hydraulic gradient in question. The main reason is that no excess pore pressure is generated at this stage with drained loading. To cover the uncertainties related to coefficient of permeability of the sand, analyses # 3.1 and # 3.2 are performed with a permeability that is 10 and 1/10 times of the reference value used in analysis # 3. It is seen that a higher permeability results in a smaller hydraulic gradient.

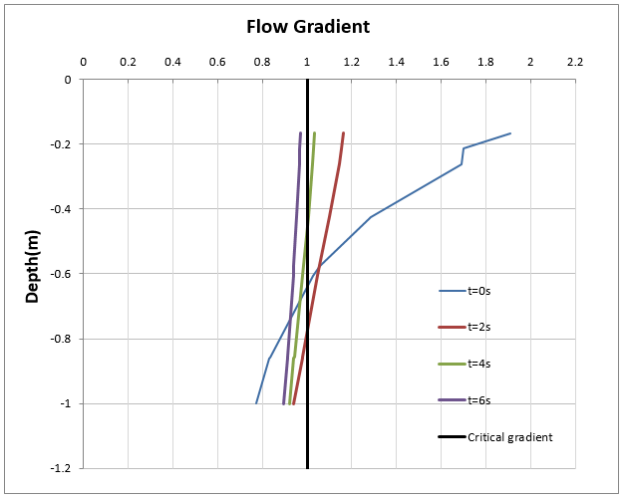

Figure 10 Hydraulic gradients- Analysis #3

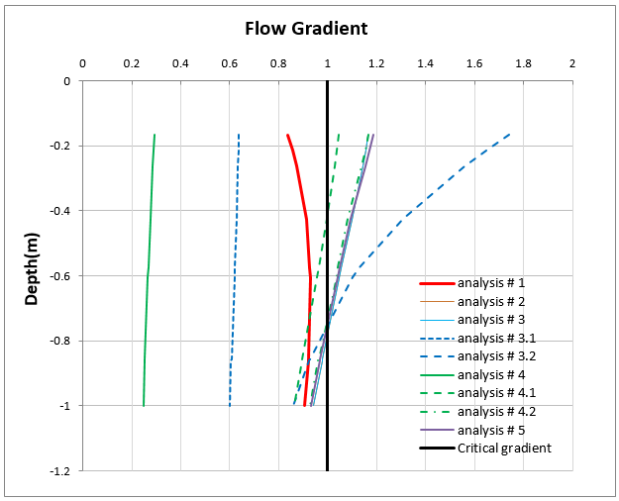

Figure 11 Summary of hydraulic gradients at t=2s

CONCLUSIONS AND DISCUSSIONS

It is seen that the high gradients close to critical gradients are limited in space, as well as in time. Gradients above 1 may start from approximately 7-8m outside the foundation to approximately 15m, extending to a depth close to 1 m at approximately 9- 10m outside the foundation. This means that the soil may become liquefied for very short time within this surface zone for the maximum wave load, but this will occur only for the very few largest waves. A gradient in the opposite direction is to be expected in the opposite phase of the wave loading. In the close vicinity of the skirts suction will be generated due to the downward motion of the foundation. This will prevent piping around the skirts to take place.

It must be emphasized that a basic assumption for the analyses is that there is no initial piping as a result of installation. It is essential that this is assured by a combination of sufficiently large diameter evacuation pipes and sufficiently low velocity of skirt penetration. There are several examples of installation of skirted foundations where significant piping has occurred as a result of too small evacuation pipes and uncontrolled penetration. It may be inevitable to have some piping at the start of penetration, but the excess pressure inside the skirts ,and the corresponding flow velocity must be sufficiently low to stop the initial piping well before reaching full penetration of the skirts. Designing the evacuation system to avoid hydraulic fracturing at full penetration for a situation of full contact between the skirt and the soil is not relevant.

REFERENCES

[1] Shazzad M.H, Investigation of Soil Failure Mechanisms during Spudcan Foundation Installation

[2] Cahuzac J, Chevallier J and Turner L., Jack-up Rigs: Evolution of Design, Oilfield Review publication, Drilling, Vol 1 (1), pp. 35-42, 1989

[3] Dean E. T. R., "A spudcan foundation model with excess pore pressures. Part 1. A principle of effective loads." Marine Structures 17(3-4), 2004, pp.219-243.

[4] Zhou X, Chow Y. K. and Leung C. F., "Numerical modelling of extraction of spudcans." Geotechnique 59(1), 2009

[5] Yang YU, Hou Lee F, Huat Goh S, Wu Jer F and Zhang Zi Y, Pore pressure generation and dissipation effects on spudcan fixity in normally consolidated clay, OMAE, paper No 10318, 2013

[6] Cuellar P, Mira P, Pastor M, Merodo J, Baebler M and Rucker W, A numerical model for the transient analysis of offshore foundations under cyclic loading, Computers and geotechnics, 59, pp 75-86

[7] Hsu Y.S, Excess pore pressure under cyclically loaded model jack-up foundations, PhD thesis, University of Cambridge, 1998

[8] Byrne B.W, Houlsby G.T and Martin C.M, Cyclic loading of shallow offshore foundations on sand, Department of Engineering Science, The university of Oxford (shared in the authors website)

[9] Tao Yi, Zhao B, Ping Y, Yang Y, Lee F, Goh S, Zhang X and Wu J, Post-installation pore-pressure changes around spudcan and long-term spudcan behaviour in soft clay, Elsevier, Computer and geotechnics, 56, pp. 133-147, 2014

[10] PlAXIS 2D, version 2017.0.0.0